

ON THE WALL BOUNDARY CONDITION FOR COMPUTING TURBULENT HEAT TRANSFER WITH $K - \omega$ MODELS

J. Bredberg *

Dept. of Thermo and Fluid Dynamics
Chalmers University of Technology
SE-412 96 Göteborg
Sweden
Email: bredberg@tfd.chalmers.se

S-H. Peng

Dept. of Thermo and Fluid Dynamics
Chalmers University of Technology
SE-412 96 Göteborg
Sweden
Email: peng@tfd.chalmers.se

L. Davidson

Dept. of Thermo and Fluid Dynamics
Chalmers University of Technology
SE-412 96 Göteborg
Sweden
Email: lada@tfd.chalmers.se

ABSTRACT

A new wall boundary condition for the standard Wilcox's $k - \omega$ model (1988) is proposed. The model combines a wall function and a low-Reynolds number approach, and a function that smoothly blends the two formulations, enabling the model to be used independently of the location of the first interior computational node. The model is calibrated using DNS-data for a channel flow and applied to a heat transfer prediction for a flow in a rib-roughened channel ($Re_b = 100\,000$). The results obtained with the new model are improved for various mesh sizes and are asymptotically identical with those of the standard $k - \omega$ turbulence model.

INTRODUCTION

The calculating performance of computers has increased so rapidly in recent years that even PCs are now commonly used to analyze complex turbulent flows. Computational Fluid Dynamics (CFD) has gone from being a field solely devoted to academic research, to becoming a useful engineering tool. However, as CFD-codes are more frequently used in industry, less time is spent on grid generating, validating results and comparing different numerical models. Although more powerful computers are becoming available, the industrial approach is usually not to refine the mesh but rather to increase the size of the problem. It is partly for this reason that the wall function method based on the $k - \epsilon$ model still prevails, although it has largely been abandoned

by many academic studies, with good physical reasoning, Launder (1984) and Patel, Rodi, and Scheuerer (1984).

A major deficiency inherent in models that utilize the law of the wall is that they are unable to predict non-equilibrium flows appearing in, e.g., separated regions to a satisfactory level of accuracy. This is particularly true for heat transfer, where the prediction is even more sensitive to the near-wall modeling, Launder (1988), and wall functions have hence received little attention lately. The model by Launder and Spalding (1974) is still the most commonly used in engineering practice. Launder's group proposed an improved model, Chieng and Launder (1980), and later corrected it, Johnson and Launder (1982), although the greater numerical complexity was not balanced by an equal enhancement of the results, see Acharya et al. (1998).

This paper revisits the wall function based on the two-equation turbulence model. The modeling approach of Chieng and Launder (1980) of introducing a viscous sublayer thickness, y_v , to divide the near-wall region into two layers, one viscous and the other turbulent, is further developed. In the present model, however, the wall functions are used with the $k - \omega$ model, Wilcox (1988), instead of the $k - \epsilon$ model, Jones and Launder (1972). This choice is made on the basis of conclusions from previous work; Peng et al. (1997), Bredberg (1999), Bredberg et al. (2000). In addition Huang and Bradshaw (1995) showed that the specific dissipation rate, ω , was the most desirable choice for the secondary turbulent quantity in a two-equation eddy-viscosity model. It is also found in this work that slightly modifying the near-wall treatment proposed by Chieng and Launder numerically simplifies the model if ω is used instead of ϵ .

*Address all correspondence to this author.

Owing to the local equilibrium assumption inherent in the wall function approach, it is unreasonable to expect any significant improvements in the predictions of complex flows such as the flow in a rib-roughened channel. The primary purpose of this study at this stage, however is, not to improve predictions using wall functions (even though a slight enhancement was achieved) but rather to establish a plausible physical and mathematical model for near-wall treatment. Hence it is desirable to bring about predictions that are reasonably accurate and relatively insensitive to the first near-wall node, no matter where in the near-wall region the first node is located. This is especially important in recirculating flows, in which it is impossible to generate grids for which the near-wall node is located in the region $30 \leq y^+ \leq 100$. The new wall boundary condition is composed of two parts, one based on the relations in the viscous sublayer and the other on those in the log layer. The partition line, the viscous sublayer thickness, y_v , is defined from the sublayer Reynolds number, $Re_v \equiv y_v \sqrt{k_v} / \nu$. The two parts are then blended together using a simple exponential function which ensures that the model behaves as a high-Reynolds number (HRN) model for a coarse mesh and gradually transforms to a low-Reynolds number (LRN) model when refining the mesh. In this paper HRN refers to the situation in which wall functions are used to bridge the near-wall region rather than resolving the variables (LRN).

The model is calibrated for a channel flow using Direct Numerical Simulation (DNS)-data, and then applied to a rib-roughened channel with heat transfer, as found in the internal cooling passages in a turbine blade. Results are presented for both cases.

THE PHYSICAL AND MATHEMATICAL MODEL

Equations of mean motion

The modeled Reynolds averaged equations for continuity, momentum and temperature are, respectively,

$$\frac{\partial \rho U_i}{\partial x_i} = 0 \quad (1)$$

$$\frac{D\rho U_i}{Dt} = -\frac{\partial P}{\partial x_i} + \frac{\partial}{\partial x_j} \left[(\mu + \mu_t) \frac{\partial U_i}{\partial x_j} \right] \quad (2)$$

$$\frac{D\rho T}{Dt} = \frac{\partial}{\partial x_i} \left[\left(\frac{\mu}{Pr} + \frac{\mu_t}{Pr_t} \right) \frac{\partial T}{\partial x_i} \right] \quad (3)$$

where $D/Dt = \partial/\partial t + U_j \partial/\partial x_j$ and the laminar and turbulent Prandtl numbers are: $Pr = 0.71$ and $Pr_t = 0.85$, Kader and Yaglom (1972).

Turbulence transport equations

The equations for the turbulent kinetic energy and specific dissipation rate are, Wilcox (1988), respectively,

$$\frac{D\rho k}{Dt} = \tau_{ij} \frac{\partial U_i}{\partial x_j} - \rho \beta^* \omega k + \frac{\partial}{\partial x_j} \left[(\mu + \sigma^* \mu_t) \frac{\partial k}{\partial x_j} \right] \quad (4)$$

$$\frac{D\rho \omega}{Dt} = \gamma \frac{\omega}{k} \tau_{ij} \frac{\partial U_i}{\partial x_j} - \rho \beta \omega^2 + \frac{\partial}{\partial x_j} \left[(\mu + \sigma \mu_t) \frac{\partial \omega}{\partial x_j} \right] \quad (5)$$

where the Boussinesq hypothesis has been applied to the Reynolds stress tensor, $\tau_{ij} = -\rho \overline{u'_i u'_j} = 2\mu_t S_{ij}$, with the turbulent viscosity defined as $\mu_t = \gamma^* \rho k / \omega$. The closure coefficients are

$$\begin{aligned} \sigma &= 1/2, & \sigma^* &= 1/2, & \beta &= 3/40 \\ \beta^* &= 9/100, & \gamma &= 5/9, & \gamma^* &= 1 \end{aligned} \quad (6)$$

Wall boundary condition

Asymptotic solution The boundary condition on a solid surface for the velocity field is the no-slip condition with an LRN grid. A constant wall heat flux is applied for the thermal field. The turbulent kinetic energy is zero at the wall, while the specific dissipation rate is set according to

$$\omega_w \rightarrow \frac{6\nu}{\beta y^2} \quad (7)$$

which is valid in the asymptotic limit of $y \rightarrow 0$.¹

Wall function approach With a coarse grid, the commonly applied approach has been to set the variables in the first near-wall node with the aid of the law of the wall, which reads

$$u^+ = \frac{U}{u_\tau} = \frac{1}{\kappa} \ln(y^+) + B \quad (8)$$

where $B = 5.1$ and $\kappa = 0.41$. $()^+$ are non-dimensionalized variables using wall quantities, u_τ, ν , where the friction velocity is defined as $u_\tau = \sqrt{\tau_w / \rho}$.

In the present study, an artificial viscosity is prescribed at the wall and the effective viscosity at the wall is then modified according to:

$$\mu_w = \mu + \frac{\rho u_\tau \kappa y}{\ln(Ey^+)} \quad (9)$$

¹According to Wilcox (1993b) Eq. (7), holds only for nodes within $y^+ < 2.5$. To establish a grid independent solution, 7-10 nodes are required in this range.

to ensure that the wall shear, $\tau_w = \mu(\partial U/\partial y)_w = \mu_w U_p/y_p$, is correct. Subscript p denotes the first interior computational node. The relations for the turbulence quantities are similarly found by solving the turbulence equations in the near-wall region. In the case of the $k - \omega$ turbulence model, these give:

$$k = \frac{u_\tau^2}{\sqrt{\beta^*}} \quad (10)$$

$$\omega = \frac{\sqrt{k}}{\beta^{*1/4} \kappa y} \quad (11)$$

Using the same approach as for the velocity field, it is possible to find a logarithmic law for the thermal boundary layer:

$$T^+ = \frac{T_w - T}{T_\tau} = \frac{1}{\kappa_T} \ln(y^+) + B_T \quad (12)$$

with $B_T \approx 3.9$ (air, $Pr = 0.71$) and $\kappa_T \approx 0.48$, Kader and Yaglom (1972), Kays and Crawford (1993), Huang and Bradshaw (1995). T_τ is the friction temperature defined as: $T_\tau = q_w/\rho c_p u_\tau$. The above relation for the wall temperature is not as common however, and it is usually expressed as:

$$T^+ = Pr_t(u^+ + Pr_{fn}) \quad (13)$$

where $Pr_{fn} = B_T/Pr_t - B$, and $Pr_t = \kappa/\kappa_T$. The constant, Pr_{fn} , depends on the Prandtl number according to Jayatillaka (1969) as:

$$Pr_{fn} = 9.24 \left[\left(\frac{Pr}{Pr_t} \right)^{3/4} - 1 \right] \left[1 + 0.28 \exp \left(-0.007 \frac{Pr_t}{Pr} \right) \right] \quad (14)$$

Integrated approach The method used in this paper is based on the approach developed by Launder *et al.* (1974), (1980), (1982), where the turbulent kinetic energy equation at the first interior node is solved rather than prescribed. This is particularly important in re-circulating flows since the law of wall is applicable only for equilibrium flow. With this approach, the terms in the turbulent kinetic energy equation must however be modified. Because the code uses a finite volume methodology, the usage of pointwise values, i.e. node value, rather than integrated values is highly questionable for a coarse mesh. This is particularly true for the production and dissipation terms in the k -equation, since both terms show a very steep variation in the near-wall region. In this model, the two turbulent quantities, k and ω , as well as the shear stress, τ_{12} , are assumed to vary in the near-wall region

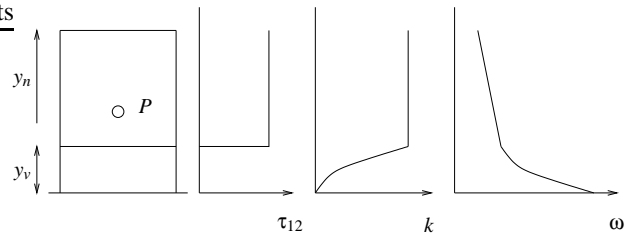


Figure 1. Assumed near-wall variation of variables.

according to Fig. 1.² The near-wall flow is treated as viscous, although not laminar in the viscous sublayer, $y < y_v$, and fully turbulent beyond that. The viscous sublayer thickness, y_v , is calculated using the sublayer Reynolds number, $Re_v \equiv y_v \sqrt{k_v}/\nu$. Chieng and Launder (1980) fixed $Re_v = 20$ at the boundary of the viscous sublayer, while Johnson and Launder (1982) showed that Re_v may be allowed to vary. The present study uses a value of 11. On the basis of DNS-data, Moser *et al.* (1999), $Re_v = 20$ is equivalent to $y^+ = 11$, which is the point at which the linear and logarithmic laws intersect. However, the viscous sublayer does not generally extend up to this value. The value used here, $Re_v = 11$, gives $y^+ = 7$, which is seen as an upper limit of the viscous sublayer.

Based on the assumed variation of the variables, the **production term**, $P = \tau_{ij} \partial U_i / \partial x_j$, is then approximated for the first node in the 2D-case as:

$$\bar{P} = \frac{1}{y_n} \left(\int_0^{y_v} \tau_{12} \frac{\partial U}{\partial y} dy + \int_{y_v}^{y_n} \tau_{12} \frac{\partial U}{\partial y} dy \right) + P' = \bar{P}_{w-v} + \tau_{12} \frac{U_n - U_v}{y_n} + P' \quad (15)$$

where the integration has been split into two parts, according to the variation shown in Fig. 1. P' denotes the contribution of the other stresses (none τ_{12}) to the production. In the case of a coarse mesh, the first term of the production could be neglected as compared with the second, since the turbulent shear stress is small in the viscous sublayer. The shear stress, τ_{12} , is assumed to be identical to the wall shear, τ_w , calculated from the logarithmic law based on the modified wall coordinates:

$$\tau_w = \frac{\kappa^* \rho U_p \sqrt{k_v}}{\ln(E^* y_p \sqrt{k_v}/\nu)} \quad (16)$$

This modified logarithmic law reduces to the conventional log-law, Eq. (8), in the limit of local equilibrium if

$$\kappa^* = \kappa \beta^{*1/4}, \quad E^* = E \beta^{*1/4} \quad (17)$$

²This variation is slightly simplified compared with those presented in Chieng and Launder (1980)

It should be noted that the wall functions used here are not the same as those proposed by Wilcox. In separated flows the logarithmic equations based on u_τ , Eqs. (8) and (12), are unsuitable for predicting heat transfer since the Nusselt number then becomes zero in separation and reattachment points, where experiments indicate the maximum level of heat transfer, see Launder (1988). By substituting u_τ with \sqrt{k} predictions for non-equilibrium flows are enhanced.

The **dissipation term** in the turbulent kinetic energy equation in the $k - \omega$ model is $\rho\varepsilon = \rho\beta^*\omega k$. In the inner region, up to y_v , the specific dissipation is assumed to vary according to the asymptotic solution, Eq. (7), while the approximation of Eq. (11) is used in the outer region. The turbulent kinetic energy is assumed to vary as $k = k_v(y/y_v)^2$ and $k = \text{const}$, respectively, giving the integrated dissipation in the two regions as

$$\rho\bar{\varepsilon}_{w-v} = \rho\beta^*\bar{\omega}k_{w-v} = \quad (18)$$

$$\frac{1}{y_v} \int_0^{y_v} \beta^* \frac{6\mu}{\beta y^2} k_v \left(\frac{y}{y_v}\right)^2 dy = \frac{\beta^* 6\mu k_v}{\beta y_v^2}$$

$$\rho\bar{\varepsilon}_{v-n} = \rho\beta^*\bar{\omega}k_{v-n} = \quad (19)$$

$$\frac{1}{y_n - y_v} \int_{y_v}^{y_n} \rho\beta^* \frac{\sqrt{k}}{\beta^{*1/4}\kappa y} k dy = \frac{\rho\beta^{*3/4}k_p^{3/2}}{\kappa(y_n - y_v)} \ln\left(\frac{y_n}{y_v}\right)$$

where k_v/y_v^2 in Eq. (18) is replaced with k_p/y_p^2 , when $y_p < y_v$. In addition the boundary condition for the **specific dissipation rate** equation must be set. The standard procedure of applying the asymptotic description as given by Eq. (7) is used for the inner region, while the integrated ω -value is used in the outer region:

$$\omega_{w-v} = \frac{6\nu}{\beta y_p^2} \quad (20)$$

$$\bar{\omega}_{v-n} = \frac{1}{y_n - y_v} \int_{y_v}^{y_n} \frac{\sqrt{k_p}}{\beta^{*1/4}\kappa y} dy = \frac{\sqrt{k_p} \ln(y_n/y_v)}{\beta^{*1/4}\kappa(y_n - y_v)} \quad (21)$$

Note that it is questionable to use the relation for the first term of the above in the limit of $y \rightarrow y_v$, where y^+ is usually too large for Eq. (7) to be valid.

The blending $k - \omega$ turbulence model All three formulations, the production terms, Eq. (15), the dissipation terms, Eqs. (18) and (19), and the boundary condition for ω , Eqs. (20) and (21), consist of one term in the inner region, $w \rightarrow v$, and another term in the outer region, $v \rightarrow n$. On the basis of this partition it would be plausible to assume that the former would be more important for a refined mesh, while the latter should be more influential for a coarse mesh. In spite of the disputable partition into two near-wall regions, the formulation benefits from an asymptotic correct description of the model in the limit of a fine mesh. While the

first term in the production, \bar{P}_{w-v} , was set to zero in Chieng and Launder (1980), which is acceptable for a coarse mesh, it should be modified in accordance with an LRN approach for a fine mesh. If the first node is located in the viscous sublayer, the production should be set according to the Boussinesq hypothesis:

$$P_{w-v} = \mu_t \left(\frac{\partial U}{\partial y}\right)^2 \quad (22)$$

Since this term increases rapidly in the buffer layer with distance to the wall, it must be controlled accordingly. In the present study, we propose to introduce a function, that reduces this term together with the inner parts of the dissipation term, Eq. (18), and boundary condition for ω , Eq. (20), for a coarse mesh, effectively changing the model to a wall function-based version of the standard $k - \omega$ model. If the function instead reduces the second terms, an LRN version of the $k - \omega$ model is recovered. Naturally the function that reduces either of the terms must be properly defined. In this paper, a simple exponential function is used:

$$f = \exp(-Re_t/C) \quad (23)$$

where $Re_t \equiv k/(\omega\nu)$ is the turbulent Reynolds number, which is preferable since it does not depend on the wall distance and is convenient to use in complex geometries. The constant, C , and the definition of the viscous sublayer thickness are optimized using DNS-data. The combination $Re_v = 11$ and $C = 1.7$ gave the overall best results, compared with the DNS-data. These values reasonably separates the LRN and HRN formulations, except in a region around $Re_v = 11$ where the function smoothly blends them, making the model independent of the first node location. The new blending $k - \omega$ turbulence model is summarized below. The production and dissipation terms in the turbulent kinetic energy equation are:

$$P = f\mu_t \left(\frac{\partial U}{\partial y}\right)^2 + (1-f)\tau_w \frac{U_n - U_v}{y_n} + P' \quad (24)$$

$$\rho\varepsilon = \rho\beta^*\omega k = f \frac{\beta^* 6\mu k_p}{\beta y_p^2} + (1-f) \frac{\rho\beta^{*3/4}k_p^{3/2}}{\kappa(y_n - y_v)} \ln\left(\frac{y_n}{y_v}\right) \quad (25)$$

The specific dissipation at the wall is set as:

$$\omega_w = f \frac{6\nu}{\beta y_p^2} + (1-f) \frac{\sqrt{k_p} \ln(y_n/y_v)}{\beta^{*1/4}\kappa(y_n - y_v)} \quad (26)$$

and the wall viscosity is set as:

$$\mu_w = f\mu + (1-f) \left[\mu + \frac{\kappa^* \rho y \sqrt{k_v}}{\ln(E^* y_p \sqrt{k_v}/\nu)} \right] \quad (27)$$

It was found that the most reasonable blending parameter for the thermal field was T^+ based on $y_k \equiv y_p \sqrt{k_p} \beta^{*1/4} / \nu$, and hence the non-dimensionalized temperature is defined as:

$$T^+ = fPr y_k + (1-f) \left[\frac{1}{\kappa_T} \ln(y_k) + B_T \right] \quad (28)$$

To achieve accurate results for heat transfer predictions when the first node is located in the buffer layer, the values of κ_T and B_T must be modified. This is not unreasonable since the constant values are valid only in the log layer. In the present model, we chose to modify only κ_T , which was reduced in the buffer layer, as found from a DNS computation, Kawamura et al. (1999). Reasonable agreement with the κ_T predicted by DNS was found for the relation:

$$\kappa_T = 0.33 [1 - \exp(-Re_t/5)] + 0.15 \quad (29)$$

which gives $\kappa_T = 0.48$ in the log layer, as indicated in experimental data.

NUMERICAL CONSIDERATIONS

A finite volume solver, CALC-BFC, Davidson and Farhanieh (1995), was employed, which solves the incompressible flow equations in a fixed Cartesian co-ordinate system. The code uses a co-located grid with boundary fitted coordinates. SIMPLE-C is used for the pressure-velocity coupling. Periodic conditions at the inlet and outlet sections are employed in this study.

RESULTS AND DISCUSSION

Channel flow

The new models constants were calibrated with channel flow DNS-data (isothermal flow, Moser et al. (1999) and thermal flow, Kawamura et al. (1999)). The Reynolds number based on the friction velocity and the channel half-height is: $Re_\tau = u_\tau h / \nu = 395$. A number of different mesh sizes was used to show the model behaviour of the first near-wall node location. The results of these computations are summarized in table 1.

The non-dimensionalized friction velocity, $u_\tau^* = 1000 \times u_\tau / U_b$ varies only slightly between the meshes, and is very similar to the DNS-data of $u_\tau^* = 57.5$, Moser et al. (1999). Included in the

nodes	10	20	40	60	80	100	100R
u_τ^*	54.9	55.0	56.4	57.4	55.7	56.9	57.6
Nu	40.3	40.3	42.2	43.4	41.6	38.9	39.4
Nu_{cf}	37.0	37.2	39.2	40.5	38.2	39.9	40.9
y_p^+	37.9	19.0	9.7	6.6	4.8	3.9	0.2
f	0	0.001	0.02	0.16	0.86	0.99	1

Table 1. Results for the DNS test case, $u_\tau^* = 1000 \times u_\tau / U_b$, $u_{\tau,DNS}^* = 57.5$, $Nu_{DB} = 41$. Number of nodes in cross-stream direction, with constant Δy except for 100R which is refined near the wall.

table is the predicted Nusselt number, $Nu \equiv hD/k$, and the Nusselt number based on a modified Reynolds analogy (Colburns analogy), $Nu_{cf} = RePr^{1/3} C_f / 2$. The Dittus-Boelter equation, $Nu_{DB} = 0.023 Re^{0.8} Pr^{0.4}$, McAdams (1942), gives $Nu_{DB} = 41$, and hence the maximum deviation for the predicted Nusselt number is merely 6%. The Colburn analogy gives similar results, however the predictions using this relation deteriorates severely in rib-roughened cases, see e.g. Bredberg et al. (2000) where C_f is shown for several turbulence models. C_f is of course trivially related to the Nusselt number when using a Reynolds analogy.

The blending function, f , only mixes the inner and outer parts in the region of $Re_v = 11$, while f is 0 and 1 in the log layer and the viscous sublayer, respectively, as it should.

The predicted velocity profiles and turbulent kinetic energy are shown in Figs. 2 and 3. The velocity profiles overlap each other with good agreement. The turbulent kinetic energy deviates in the center of the channel, however yield improved agreement in the near wall region as compared with the standard $k - \omega$ model (100R mesh). The near-wall turbulent kinetic energy is crucial when calculating heat transfer and wall friction, and hence much more important than the mesh dependency and off wall discrepancies in the predicted k . It should also be noted that the region of the peak production of turbulent kinetic energy, $y^+ = 15$, is notoriously difficult to model, and a number of damping functions is generally necessary to get the correct maxima of k^+ , see e.g. Patel et al. (1984). Because no effort has been made to correct any of the secondary variables, k and ω , apart from the simple blending function, the results are very encouraging, especially the mean quantities; $u, Nu, C_f(u_\tau)$.

Rib-roughened channel

The second study case is a rib-roughened channel, which can be found in the internal cooling channels of gas turbine blades. The geometry of this test case is shown in Fig. 4, with $P/e = 10$ and $H/e = 10$. The Reynolds number based on the bulk velocity and the channel height is $Re_b = 100\,000$. Constant heat flux was applied to the upper and lower wall, with the rib itself ther-

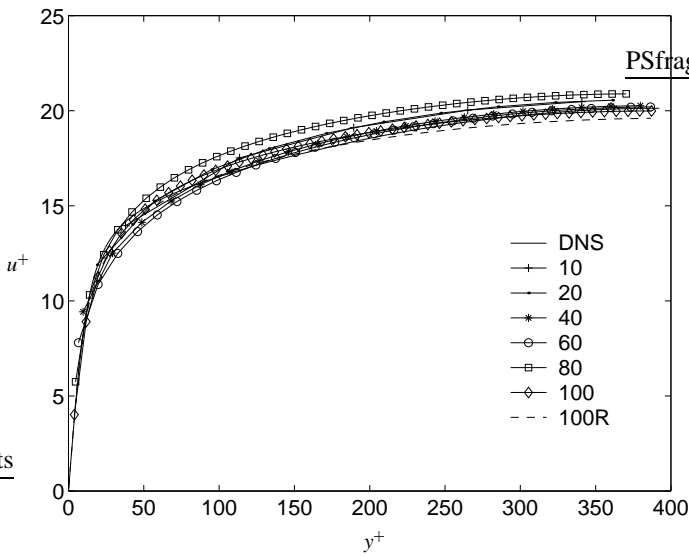


Figure 2. Velocity profile, channel flow

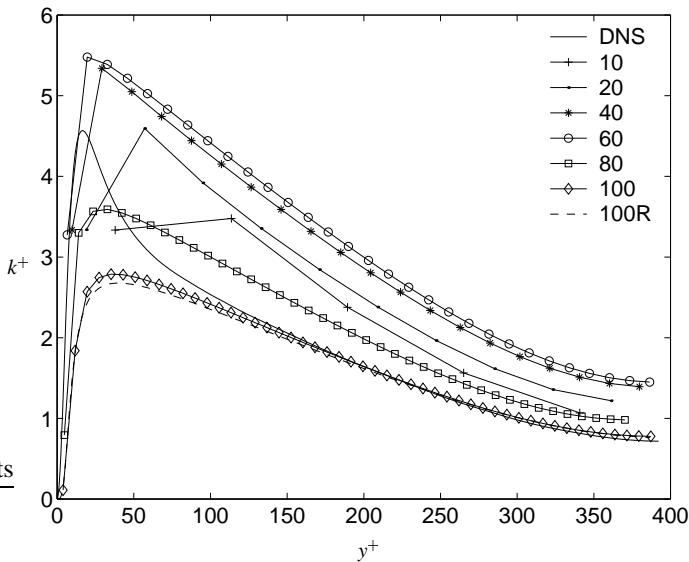


Figure 3. Turbulent kinetic energy, channel flow

mally isolated. The predictions are compared with an experiment by Nicklin (1998). Regrettably, only heat transfer measurements were performed in this experiment. However, as the near-wall behaviour of the new model is the main concern of this study, heat transfer comparisons would be most revealing. The present model is compared with other models in two cases: when the mesh is fine enough to enable an LRN-type of turbulence model prediction (LRN-case) and a coarser mesh which necessitates an HRN-type (or wall function based) turbulence model (HRN-case). In the HRN-case, the new model is compared with the

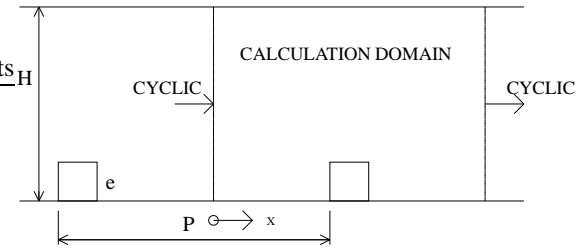


Figure 4. Rib-roughened geometry

standard Wilcox $k - \omega$ model (1988) and the Launder-Spalding $k - \epsilon$ model (1974), both adopting their respective wall functions with the Jayatillaka (1969) temperature wall function, Eq. (13). For the LRN-case, the obvious choice is to compare the new model with the predictions using the standard Wilcox $k - \omega$ model (1988), which is integrated to the wall. If the new model predict similar or better results as compared with the standard models in both cases, the purpose of the model is achieved. It should here be clearly stressed that very accurate heat transfer results are not the justification of the present model, but rather overall reasonable results independent of the location of the first near-wall node.

The predicted Nusselt numbers along the upper smooth wall are shown in Figs. 5 and 7, while those for the lower rib-roughened wall are shown in Figs. 6 and 8. The labels are denoted according to the location of the first node, non-dimensionalized with the channel height, $\eta_p = 1000 \times y_p/H$, and the models used, the present model (P), Launder-Spalding model (LS) and the Wilcox model (W). The meshes used in the HRN-case are: 20×20 and 40×40 , while those in the LRN-case are: 50×55 , 55×60 and 110×120 . The two coarsest meshes use a uniform distribution of the nodes, while the others refine the nodes close the walls. The finest mesh is refined enough to yield grid-independent results, Bredberg (1999).

In the case of a fine mesh, the new model and the Wilcox $k - \omega$ model reach the same grid-independent results, with the lines overlaying each other for the $\eta_p = 0.1$ mesh. When the mesh is made coarser, both models predict reasonable results for $y_p^+ < 1$. If the first node is located further from the wall, a calculation using the standard $k - \omega$ model is difficult to converge ($\eta_p = 4.5$ mesh) and, if a solution is found, the heat transfer is severely over predicted, as seen in the $\eta_p = 1.3$ case. This is particular true for the upper wall, where the y_p^+ is well outside the viscous sublayer for the $\eta_p = 1.3$ case, resulting in a Nusselt number exceeding 10000 (the results are not shown but only indicated in Fig. 5). For the different meshes used here, the predicted heat transfer with the new model always stays bounded. Although the model under predicts the Nusselt number, especially on the lower wall, the results remain reasonable and better than the standard $k - \omega$ when the mesh is made coarser.

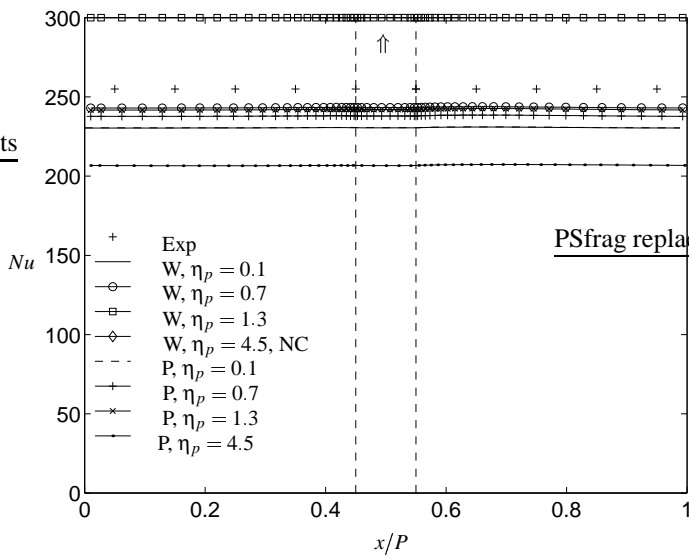


Figure 5. Nusselt number along upper wall, fine meshes (LRN-case). P, present model and W, Wilcox model. η_p is the non-dimensionalized distance to the wall. NC, non-converged result (not shown).

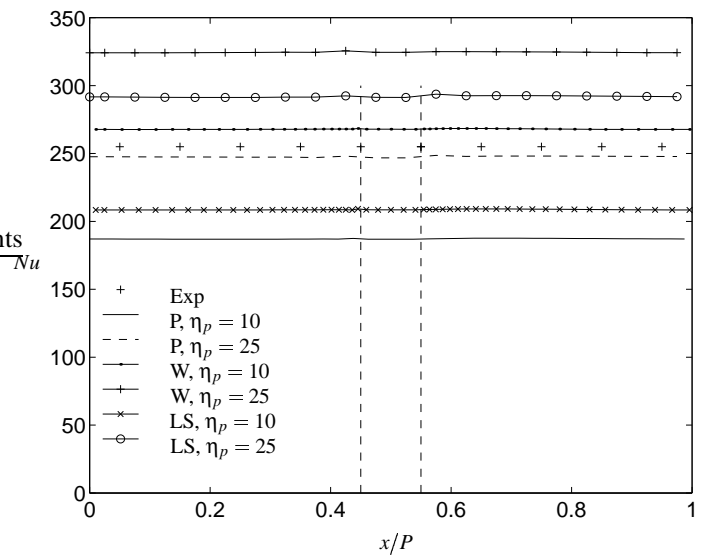


Figure 7. Nusselt number along upper wall, coarse meshes (HRN-case) P, present model, W, Wilcox model and LS, Launder-Spalding model. η_p is the non-dimensionalized distance to the wall.

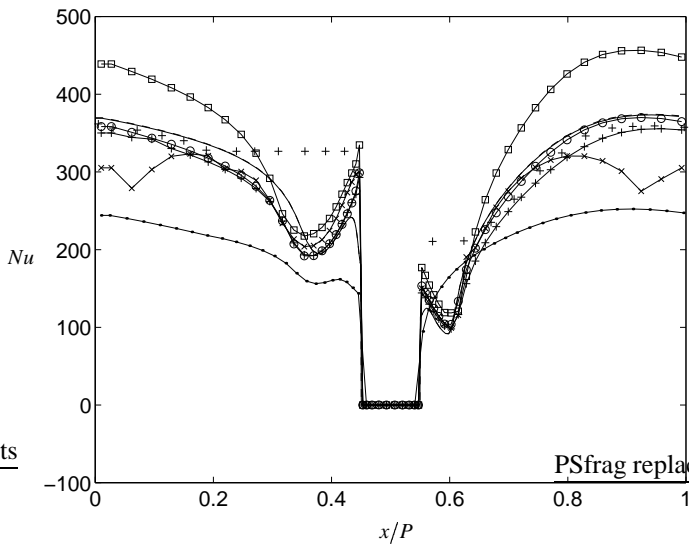


Figure 6. Nusselt number along lower wall, fine meshes (LRN-case), same labels as in Fig. 5

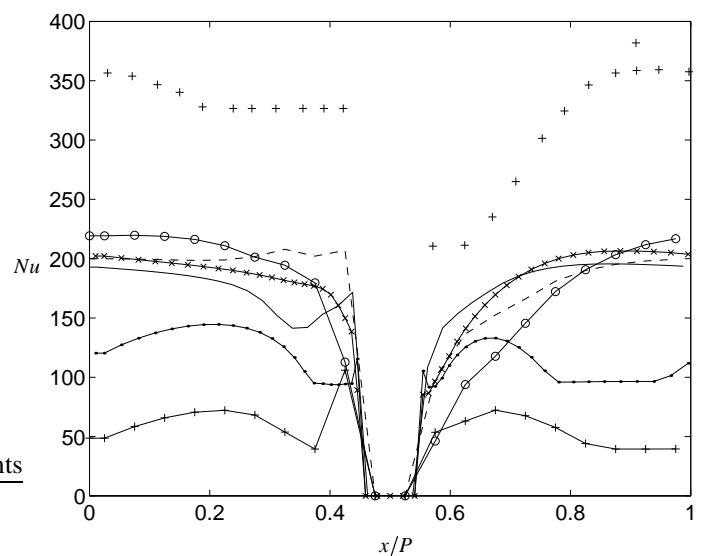


Figure 8. Nusselt number along lower wall, coarse meshes (HRN-case), same labels as in Fig. 7

In the case of a coarse mesh, Figs. 7 and 8, the new model employs the modified wall function approach, with results comparable with those of the Launder-Spalding model. This is not surprising since the two models are similar in that they solve the k -equation and fix either the ω - or ϵ -equation. Regrettably the results does not improve for the finer mesh ($\eta_p = 10$) with either of the models. The reason for this is probably the excessively low y_p^+ value on the lower wall for both meshes. Thus it is

questionable to use any model that employs wall functions in a rib-roughened channel.

The Wilcox $k - \omega$ model with the conventional wall functions seems unsuitable for heat transfer predictions in re-circulating flows (see Fig. 8), and hence it is obviously more attractive, although still erroneous, to use the Launder-Spalding methodology, as adopted in the present model.

CONCLUSIONS

A new approach for handling the wall boundary condition when using the standard $k - \omega$ model (1988) is developed and tested for a channel and a rib-roughened duct flow. The new model gives results identical to those of the $k - \omega$ model in the limit of a fine mesh and greatly improves the results for a coarse mesh as compared with the same model employing conventional wall functions. The predicted heat transfer in the rib-roughened channel stays bounded regardless of the mesh used, which enables the model to be used independently of any mesh, greatly reducing the grid-generating process. The closest agreement with experimental data was achieved with a fine mesh, with gradually larger discrepancies when the mesh was made coarser, although it was always superior to the standard $k - \omega$ model using wall functions. Future work will involve further tuning of the blending function, particularly for the temperature relation. A change of the turbulence model to the LRN version of the $k - \omega$ model (1993a), will also be studied.

ACKNOWLEDGMENTS

The present work was supported by the Swedish Gas Turbine Center.

REFERENCES

- Acharya, S., S. Dutta, and T. Myrum (1998). Heat transfer in turbulent flow past a surface-mounted two-dimensional rib. *J. Heat Transfer* 120, 724–734.
- Bredberg, J. (1999). Prediction of flow and heat transfer inside turbine blades using EARSM, $k - \epsilon$ and $k - \omega$ turbulence models. Report, Department of Thermo and Fluid Dynamics, Chalmers University of Technology, Gothenburg. Also available at www.tfd.chalmers.se/~bredberg.
- Bredberg, J., L. Davidson, and H. Iacovides (2000). Comparison of near-wall behavior and its effect on heat transfer for $k - \omega$ and $k - \epsilon$ turbulence models in rib-roughened 2D channels. In K. H. Y. Nagano and T. Tsuji (Eds.), *3:rd Int. Symposium on Turbulence, Heat and Mass Transfer*, pp. 381–388. Aichi Shuppan.
- Chieng, C. and B. Launder (1980). On the calculation of turbulent heat transfer transport downstream an abrupt pipe expansion. *Num Heat Transfer* 3, 189–207.
- Davidson, L. and B. Farhanieh (1995). CALC-BFC. Report 95/11, Department of Thermo and Fluid Dynamics, Chalmers University of Technology, Gothenburg.
- Huang, P. and P. Bradshaw (1995). Law of the wall for turbulent flows in pressure gradients. *AIAA Journal* 33, 624–632.
- Jayatillaka, C. (1969). The influence of Prandtl number and surface roughness on the resistance of the laminar sublayer to momentum and heat transfer. *Progr. in Heat and Mass Transfer* 1, 193.
- Johnson, R. and B. Launder (1982). Discussion of: On the calculation of turbulent heat transfer transport downstream an abrupt pipe expansion. *Num Heat Transfer* 5, 493–496.
- Jones, W. and B. Launder (1972). The prediction of laminarization with a two-equation model of turbulence. *Int. J. Heat and Mass Transfer* 15, 301–314.
- Kader, B. and A. Yaglom (1972). Heat and mass transfer laws for fully turbulent wall flows. *Int. J. Heat and Mass Transfer* 15, 2329–2351.
- Kawamura, H., H. Abe, and Y. Matsuo (1999). DNS of turbulent heat transfer in channel flow with respect to Reynolds and Prandtl number effects. *Int. J. Heat and Fluid Flow* 20, 196–207.
- Kays, W. and M. Crawford (1993). *Convective Heat and Mass Transfer*. McGraw-Hill, Inc.
- Launder, B. (1984). Numerical computation of convective heat transfer in complex turbulent flows: Time to abandon wall functions. *Int. J. Heat and Mass Transfer* 27, 1485–1491.
- Launder, B. (1988). On the computation of convective heat transfer in complex turbulent flows. *J. Heat Transfer* 110, 1112–1128.
- Launder, B. and D. Spalding (1974). The numerical computation of turbulent flows. *Comp methods in app. mech and eng.* 3, 269–289.
- McAdams, W. (1942). *Heat Transmission* (2nd ed.). McGraw-Hill, New York.
- Moser, R., J. Kim, and N. Mansour (1999). Direct numerical simulation of turbulent channel flow up to $Re=590$. *Phys. Fluids* 11, 943–945. Data available at www.tam.uiuc.edu/Faculty/Moser/.
- Nicklin, G. J. E. (1998). Augmented heat transfer in a square channel with asymmetrical turbulence promotion. Final year project report, Dept. of Mech. Eng., UMIST, Manchester.
- Patel, V., W. Rodi, and G. Scheuerer (1984). Turbulence models for near-wall and low Reynolds number flows: a review. *AIAA Journal* 23, 1308–1319.
- Peng, S.-H., L. Davidson, and S. Holmberg (1997). A modified low-Reynolds-number $k - \omega$ model for recirculating flows. *J. Fluid Engineering* 119, 867–875.
- Wilcox, D. (1988). Reassessment of the scale-determining equation for advanced turbulence models. *AIAA Journal* 26, 1299–1310.
- Wilcox, D. (1993a). Comparison of two-equation turbulence models for boundary layers with pressure gradient. *AIAA Journal* 31, 1414–1421.
- Wilcox, D. (1993b). *Turbulence Modeling for CFD*. DCW Industries, Inc.